# Cyclopropanation of Cyclohexenone by Diazomethane Catalyzed by Palladium Diacetate: Evidence for the Formation of Palladium(0) Nanoparticles

Ona Illa,[†] Cristóbal Rodríguez-García,[†] Carles Acosta-Silva,[†] Isabelle Favier,[‡] David Picurelli,[‡] Antonio Oliva,[†] Montserrat Gómez,*[,‡,§] Vicenç Branchadell,*[,†] and Rosa M. Ortuño*[,†]

*Departament de Química, Universitat Autònoma de Barcelona, 08193 Bellaterra, Barcelona, Spain, Departament de Química Inorgànica, Universitat de Barcelona, Martí i Franquès, 1-11, 08028 Barcelona, Spain, and Laboratoire Hétérochimie Fondamentale et Appliquée, UMR CNRS 5069, 118 Route de Narbonne, 31062 Toulouse Cedex 9, France*

*Received February 13, 2007*

The diazomethane-mediated cyclopropanation of cyclohexenone using $Pd(OAc)_2$ and different sources of Pd(0) species as precatalysts has been studied. In the presence of an excess of diazomethane, $Pd(OAc)_2$ rapidly evolves to the formation of palladium nanoparticles (less than 1 min), which are active as catalysts in the cyclopropanation process. The nature of these particles has been analyzed through transmission electron microscopy showing a size distribution between 6 and 40 nm. These nanoparticles generated in situ are more active than Pd(0) complexes, preformed nanoparticles, and commercial palladium powder. Cyclic voltammetry measurements of the reaction solution after completion show the presence of Pd(0) species. This is the first time that Pd(0) nanoparticles are evidenced in a cyclopropanation reaction. Moreover, the reduction of $Pd(OAc)_2$ to Pd(0) in the presence of diazomethane has been theoretically studied through density functional calculations. The formation of methyl and allyl acetates as organic byproducts has been predicted by the theoretical calculations, and these species, as well as oligomers derived from them, have been detected by spectrometric and spectroscopic techniques (MS, NMR, and IR).

## Introduction

For metal-catalyzed processes, many studies have been reported to establish the true nature of the catalyst. From the point of view of the reactivity, it is more appropriate to classify catalysts as homogeneous or heterogeneous depending on whether the substrate interacts with one or many types of active sites.[1] Recently, tests commonly used to evaluate the nature of the catalyst have been reviewed.[2,3] However, when metal nanoparticles are involved, it is even more difficult to conclude about the catalyst nature, because they are placed at the frontier between classical homogeneous and heterogeneous catalysts.[4]

This dilemma has been found in many palladium-catalyzed reactions.[5,6] In the last years, the possible formation of palladium nanoparticles has been postulated for several catalytic processes.[7,8] In particular, for Pd-catalyzed C−C coupling reactions,[9] palladium nanoparticles seem to act as a reservoir of molecular palladium species, as proposed by Dupont[10] and in agreement with the results obtained by de Vries using ligand-free palladium catalysts.[11]

Cyclopropanation of olefins with diazoalkanes catalyzed by metal complexes is a widely used synthetic method.[12−29]

* Corresponding authors. E-mail: (M.G.) gomez@chimie.ups-tlse.fr; (V.B.) vicenc@klingon.uab.cat; (R.M.O.) rosa.ortuno@uab.es.
[†] Universitat Autònoma de Barcelona.
[‡] Universitat de Barcelona.
[§] Laboratoire Hétérochimie Fondamentale et Appliquée.

(1) Schwartz, J. *Acc. Chem. Res.* **1985**, *18*, 302.
(2) Widegren, A.; Finke, R. G. *J. Mol. Catal. A: Chem.* **2003**, *198*, 317.
(3) Dyson, P. J. *Dalton Trans.* **2003**, 2964.
(4) Astruc, D.; Lu, F.; Ruiz Aranzaes, J. *Angew. Chem., Int. Ed.* **2005**, *44*, 7852.
(5) Amatore, C.; Jutand, A. *Acc. Chem. Res.* **2000**, *33*, 314.
(6) Phan, N. T. S.; Van Der Sluys, M.; Jones, C. W. *Adv. Synth. Catal.* **2006**, *348*, 609.
(7) de Vries, J. G. *Dalton Trans.* **2006**, 421.
(8) Thathagar, M. B.; ten Elshof, J. E.; Rothenberg, G. *Angew. Chem., Int. Ed.* **2006**, *45*, 2886.
(9) For a general review concerning the Pd catalyst nature in Heck and Suzuki couplings, see: Phan, N. T. S.; van der Sluys, M.; Jones, C. W. *Adv. Synth. Catal.* **2006**, *348*, 609.
(10) Cassol, C. C.; Umpierre, A. P.; Machado, G.; Wolke, S. I.; Dupont, J. *J. Am. Chem. Soc.* **2005**, *127*, 3298.
(11) (a) Reetz, M. T.; de Vries, J. G. *Chem. Commun.* **2003**, 1787. (b) de Vries, A. H. M.; Mulders, J. M. C. A.; Mommers, J. H. M.; Henderickx, H. J. W.; de Vries, J. G. *Org. Lett.* **2003**, *5*, 3285.
(12) Doyle, M. P. *Chem. Rev.* **1986**, *86*, 919.
(13) Tomilov, Y. V.; Dokichev, V. A.; Dzhemilev, U. M.; Nefedov, O. M. *Russ. Chem. Rev.* **1993**, *62*, 799.
(14) Doyle, M. P. In *Comprehensive Organometallic Chemistry 2, Vol 12*; Hegedus, L. S., Ed.; Pergamon: New York, 1995; p 387.
(15) Lautens, M.; Klute, W.; Tam, W. *Chem. Rev.* **1996**, *96*, 49.
(16) Davies, H. M. L. *Aldrichim. Acta* **1997**, *30*, 107.
(17) Doyle, M. P.; Protopopova, M. N. *Tetrahedron* **1998**, *54*, 7919.
(18) Doyle, M. P.; Forbes, D. C. *Chem. Rev.* **1998**, *98*, 911.
(19) Herndon, J. W. *Coord. Chem. Rev.* **2000**, *206*, 237.
(20) Lebel, H.; Marcoux, J.-F.; Molinaro, C.; Charette, A. B. *Chem. Rev.* **2003**, *103*, 977.
(21) Paulissen, R.; Hubert, A. J.; Teyssié, P. *Tetrahedron Lett.* **1972**, 1465.
(22) Mende, U.; Radüchel, B.; Skuballa, B.; Vorbrüggen, H. *Tetrahedron Lett.* **1975**, 629.
(23) Kottwitz, J.; Vorbrüggen, H. *Synthesis* **1975**, 636.
(24) Suda, M. *Synthesis* **1981**, 714.
(25) Anciaux, A. J.; Hubert, A. J.; Noels, A. F.; Petinot, N.; Teyssié, P. *J. Org. Chem.* **1980**, *45*, 695.
(26) Ortuño, R. M.; Ibarzo, J.; Álvarez-Larena, Á.; Piniella, J. F. *Tetrahedron Lett.* **1996**, *37*, 4059.
(27) Denmark, S. E.; Stavenger, R. A.; Faucher, A. M.; Edwards, J. P. *J. Org. Chem.* **1997**, *62*, 3375.

10.1021/om070141a CCC: $37.00 
Publication on Web 05/27/2007

Palladium diacetate has been shown to be an efficient catalyst in the diazomethane-mediated cyclopropanation of different kinds of olefins.[21−29] Nevertheless, the mechanism of the reaction is still controversial and not completely understood. It is currently assumed that the first step involves the formation of a palladium−carbene complex, resulting from the reaction between the palladium(II) complex and diazomethane.[12,27] The interaction of the olefin with this complex could lead to the formation of a palladacyclobutane intermediate.

The ability of palladium to coordinate olefins has led to the postulation of an alternative mechanism in which diazomethane attacks a previously coordinated olefin.[25] Tomilov et al.[13] have suggested that the catalytically active species is a Pd(0) complex, which would be produced from the reduction of palladium(II) compounds in the presence of diazomethane. Actually, the precipitation of palladium black has been observed from the reaction between Pd(II) compounds and diazomethane.[13,30,31]

The transition-metal-catalyzed cyclopropanation of olefins has been the subject of theoretical studies.[32−41] We have studied the cyclopropanation of ethylene by diazomethane using palladium diformate as a model of palladium diacetate.[34] Accordingly, the cyclopropanation is possible only after the reaction of palladium diformate with two diazomethane molecules to form a bis(formyloxymethyl)palladium complex in which two methylene groups have been inserted into Pd−O bonds. The coordination of the third diazomethane molecule initiates the catalytic cycle, in which the highest transition state is the one corresponding to nitrogen elimination (Gibbs energy: 23.7 kcal $mol^{-1}$ at 298.15 K with respect to [Pd(formyloxymethyl)$_2$] + diazomethane).

Bernardi et al.[35] have theoretically studied the cyclopropanation of ethylene in the presence of [$PdCl_2(PH_3)_2$] and have shown that the catalytically active species is a carbenoid complex in which methylene has inserted into one of the Pd−Cl or Pd−P bonds. The most favorable cyclopropanation pathway involves activation barriers of 28−29 kcal $mol^{-1}$.

On the other hand, Straub[37] has reported a theoretical study on the mechanism of cyclopropanation of ethylene by diazomethane catalyzed by [Pd(ethylene)$_n$] ($n$ = 1, 2, 3) complexes. The highest point along the reaction coordinate is the transition state corresponding to nitrogen elimination (Gibbs energy: 20.1 kcal $mol^{-1}$ at 273.15 K with respect to [Pd(ethylene)$_2$] + diazomethane). These results show that Pd(0) complexes may be more efficient catalysts for the cyclopropanation of olefins than Pd(II) complexes. However, the mechanism for the Pd(II) to Pd(0) reduction remains unclear.

**Scheme 1**

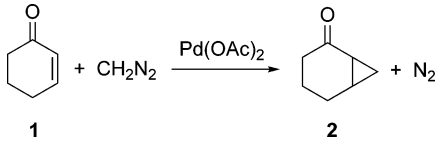


**1** **2**

**Scheme 2**

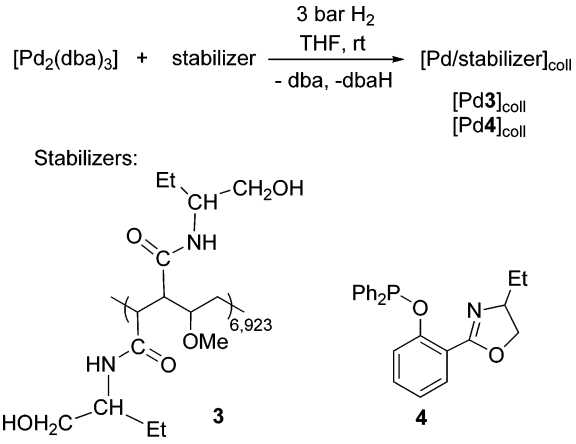


In the present paper, we report the results of our investigation on the cyclopropanation of cyclohexenone by diazomethane using $Pd(OAc)_2$ or Pd(0) compounds as catalytic precursors. The palladium species formed have been analyzed, during and/or after the reaction, both in the solid state (by transmission electron microscopy (TEM) and far-IR spectroscopy) and solution (by cyclic voltammetry). Furthermore, the mechanism of Pd(II) to Pd(0) reduction has been studied through density functional theoretical (DFT) calculations, which have allowed the prediction of the byproducts resultant from such a process; their formation has been experimentally confirmed by mass spectrometry and spectroscopic techniques.

## Results and Discussion

**1. Pd-Catalyzed Cyclohexenone Cyclopropanation.** The reaction between cyclohexenone **1** and diazomethane catalyzed by $Pd(OAc)_2$ to afford bicylo[4.1.0]heptan-2-one, **2**, was studied as a model reaction (Scheme 1).

In our earlier studies,[26,28] we demonstrated that a large excess (ca 20 equiv) of diazomethane is necessary to achieve an efficient cyclopropanation in a few minutes. Upon addition of diazomethane to the solution of **1** and $Pd(OAc)_2$, an immediate production of nitrogen and formation of Pd(0) were observed. After completion, the palladium formed was exhaustively washed to remove organic materials and reused in a further reaction obtaining a 1:1 mixture of cyclohexenone **1** and cyclopropane **2**.

The reactant addition sequence is crucial: only a very low conversion was observed when cyclohexenone was poured into a mixture containing the catalyst and diazomethane, in contrast to the high conversion obtained when the diazomethane is poured into the cyclohexenone solution containing palladium diacetate.

After these preliminary observations and with the aim of obtaining more experimental data about the nature of the palladium catalytic species involved in the cyclohexenone

(28) Rodríguez-García, C.; Ibarzo, J.; Álvarez-Larena, A.; Branchadell, V.; Oliva, A.; Ortuño, R. M. *Tetrahedron* **2001**, *57*, 1025.
(29) Marko, I. E.; Giard, T.; Sumida, S.; Gies, A.-E. *Tetrahedron Lett.* **2002**, *43*, 2317.
(30) McCrindle, R.; Arsenault, G. J.; Farwaha, R.; McAlees, A. J.; Sneddon, D. W. *J. Chem. Soc., Dalton Trans.* **1989**, 761.
(31) Vallgårda, J.; Appleberg, U.; Csöregh, I.; Hacksell, U. *J. Chem. Soc., Perkin Trans. 1* **1994**, 461.
(32) Rodríguez-García, C.; González-Blanco, O.; Oliva, A.; Ortuñno, R. M.; Branchadell, V. *Eur. J. Inorg. Chem.* **2000**, 1073.
(33) Bernardi, F.; Bottoni, A.; Miscioni, G. P. *Organometallics* **2000**, *19*, 5529.
(34) Rodríguez-García, C.; Oliva, A.; Ortuñno, R. M.; Branchadell, V. *J. Am. Chem. Soc.* **2001**, *123*, 6157.
(35) Bernardi, F.; Bottoni, A.; Miscioni, G. P. *Organometallics* **2001**, *20*, 2751.
(36) Fraile, J. M.; García, J. I.; Martínez-Merino, V.; Mayoral. J. A.; Salvatella, L. *J. Am. Chem. Soc.* **2001**, *123*, 7616.
(37) Straub, B. F. *J. Am. Chem. Soc.* **2002**, *124*, 14195.
(38) Straub, B. F.; Gruber, I.; Rominger, F. Hofmann, P. *J. Organomet. Chem.* **2003**, *684*, 124.
(39) Iwakura, I.; Ikeno, T.; Yamada, T. *Org. Lett.* **2004**, *6*, 949.
(40) Fraile, J. M.; García, J. I.; Gil, M. J.; Martínez-Merino, V.; Mayoral, J. A.; Salvatella, L. *Chem.−Eur. J.* **2004**, *10*, 758.
(41) Cornejo, A.; Fraile, J. M.; García, J. I.; Gil, M. J.; Martínez-Merino, V.; Mayoral, J. A.; Salvatella, L. *Organometallics* **2005**, *24*, 3448.

**Table 1. Cyclopropanation of Cyclohexenone 1 by Diazomethane to Afford 2, Using Different Palladium Precatalysts**

| entry | Pd precatalyst | Pd/**1**/$CH_2N_2$[a] | time[b] | **1**/**2**[c] |
|---|---|---|---|---|
| 1 | $Pd(OAc)_2$ | 1/1/20 | 5 | 10/90 |
| 2 | $Pd_2(dba)_3$ | 1/1/20 | 5 | 50/50 |
| 3 | $Pd(PPh_3)_4$ | 1/1/20 | 10 | 100/0 |
| 4 | Pd(s)[d] | 1/1/20 | 5 | 60/40 |
| 5 | $[Pd3]_{coll}$ | 1/1/20 | 240 | 100/0 |
| 6 | $[Pd4]_{coll}$ | 1/1/20 | 180 | 100/0 |
| 7 | $Pd(OAc)_2$ + dba (Pd/dba = 1/3) | 1/1/20 | 5 | 60/40 |
| 8 | $Pd(OAc)_2$ + $PPh_3$ ($Pd/PPh_3$ = 1/4) | 1/1/20 | 5 | 100/0 |
| 9 | $Pd(OAc)_2$ | 0.1/1/20 | 5 | 25/75 |

[a] Initial relative concentrations. [b]Reaction time in minutes. [c]Determined by GC. [d] Commercial palladium black.

cyclopropanation (Scheme 1), we decided to study this process using other palladium sources. In particular, we have used $Pd_2(dba)_3$ and $Pd(PPh_3)_4$, as typical molecular precursors, Pd(0) sponge, as a typical heterogeneous catalyst, and preformed palladium nanoparticles, $[Pd3]_{coll}$ and $[Pd4]_{coll}$ using a functionalized polymer (**3**), which is a classical method to isolate nanoparticles,[42] and a ligand (**4**), respectively (Scheme 2).[43] This choice was done to observe the influence of both kinds of stabilizers in the reactivity herein considered. In all cases, diazomethane was poured into a dichloromethane solution containing cyclohexenone and the palladium compound at room temperature, and the results are summarized in Table 1.

The comparison of the results obtained under the same reaction conditions (entries 1−6, Table 1) shows that palladium diacetate presents the highest activity, giving 90% conversion in 5 min (entry 1). The activity of $Pd_2(dba)_3$ is worse than $Pd(OAc)_2$, giving only 50% conversion (entry 2). This result is similar to that obtained when dba is added to palladium diacetate (entry 7). In this case, mono- and bis-cyclopropanation of the two double bonds of dba were also observed, so that dba cyclopropanation competes with cyclohexenone cyclopropanation.

It is noteworthy the lack of activity of $Pd(PPh_3)_4$ (entry 3) and of the preformed nanoparticles (entries 5 and 6). The strong Pd−phosphine interaction in $Pd(PPh_3)_4$ probably prevents the creation of vacant coordination sites for diazomethane or cyclohexenone. In fact, when 4 equiv of $PPh_3$ was added to $Pd(OAc)_2$, no cyclopropanation at all was observed (entry 8) and the $^{31}P$ NMR spectrum of the reaction mixture revealed the formation of $Ph_3PO$ (25 ppm) and $Pd(PPh_3)_4$ (22 ppm). These results are in accordance with those previously described by Jutand et al.[44] on the reduction of Pd(II) to Pd(0) by triphenylphosphine as reducing agent.

The behavior of the preformed nanoparticles has been investigated by TEM analysis. In the case of nanoparticles stabilized by polymer, $[Pd3]_{coll}$, agglomeration was observed after 5 min of reaction time (Figure 1), leading to a diminution of the active surface. The lack of activity in the cyclopropanation may be due to the coordination of Lewis base centers to the active sites in the surface. On the contrary, the size of the nanoparticles sterically stabilized by the oxazolinyl−phosphinite, $[Pd4]_{coll}$, remained unaltered (Figure 2). In this case, it seems that the stabilizing ligand also prevents the approach of cyclohexenone and/or diazomethane to the metal surface.

For the best precatalyst used, cyclopropanation of **1** was also carried out using a lower Pd/substrate ratio (0.1/1, entry 9) and 75% of cyclopropane **2** was obtained, showing the palladium catalytic role.

In view of these results, we decided to study more exhaustively $Pd(OAc)_2$ as a catalytic precursor of cyclohexenone cyclopropanation.

With the purpose of monitoring the diazomethane decomposition, 1 equiv of $Pd(OAc)_2$ and 20 equiv of diazomethane were stirred in dichloromethane at −80 °C. After 5 min, when all initial diazomethane had already disappeared and presumably all $Pd(OAc)_2$ had been reduced, 20 more equivalents of diazomethane were added to the reaction mixture and the stirring was continued for an additional 4 min. Figure 3 shows the variation of diazomethane concentration after the two additions of diazomethane. After the first addition, the diazomethane concentration decreased to 50% in only 30 s, whereas after the second addition, the time necessary to reach the same diminution was more than 1 min. Therefore, the diazomethane disappearance is faster for the first addition than for the second one.

This fast decomposition of diazomethane by $Pd(OAc)_2$ explains why very low or no conversion was observed when cyclohexenone was added to a mixture containing diazomethane and $Pd(OAc)_2$ in dichloromethane or ether.

The organic species resulting from decomposition of $Pd(OAc)_2$ by diazomethane were analyzed by electrospray ionization (ESI) mass spectrometry, revealing the presence of significant signals. For instance, a peak attributable to $CH_3C(O)OCH_3$ was observed at *m*/*z* 74, and signals at *m*/*z* 100 + 14*n* corresponding to $CH_3C(O)O(CH_2)_nCH{=}CH_2$ were also detected. Furthermore, other peaks with masses fitting well to a $CH_3C(O)O(CH_2)_nOC(O)CH_3$ structure (132 + 14*n*) were identified. In addition, $^1H$ NMR and IR spectra of a sample corresponding to 0.5 min reaction time corroborated these structures. Thus the $^1H$ NMR spectrum in $CDCl_3$ showed signals at $\delta$ 1.5 and 1.8 ($CH_2$), 2.0 ($CH_3C{=}O$), 3.7 ($CH_3OC{=}O$), 4.1 ($CH_2OC{=}O$), 4.7 ($C{=}C-CH_2OC{=}O$ and vinyl protons), 4.9, 5.3, and 5.4 (several *cis/trans* vinyl protons), and 7.3 ($CH_2{=}CHOC{=}O$) ppm, compatible with the proposed structures. Concerning the IR spectrum, absorptions at 1578 and 1635 (C=C) and 1720 (C=O) $cm^{-1}$ were observed.

Under cyclopropanation conditions, a black precipitate is always observed using palladium acetate as precursor. In order to know the nature of the insoluble palladium species formed, TEM analyses were carried out (Figure 4). For the cyclopropanation using a 1/1 Pd/**1** ratio (entry 1, Table 1), small palladium particles (mean diameter ca. 5 nm) forming agglomerates were observed (Figure 4a). On the other hand, bigger nanoparticles were detected when the Pd/**1** ratio was 0.1/1 (entry 9, Table 1), showing two populations at ca. 26 and 40 nm (Figure 4b).

With the aim of proving the catalytic role of the Pd nanoparticles, the reaction was carried out at −80 °C and monitored by TEM and GC. A 1/20 mixture of $Pd(OAc)_2$ and diazomethane in dichloromethane at −80 °C was stirred for 5 min, and then 1 equiv of cyclohexenone and an additional 15 equiv of diazomethane were added. After 6 min (overall time), 95% cyclopropane **2** was determined by GC. The black solid formed during the catalytic reaction was analyzed by TEM (Figure 5), showing the presence of nanoparticles that increased

(42) Schmid, G., Ed. *Nanoparticles. From theory to application*; Wiley-VCH: Weinheim, 2004.

(43) Palladium nanoparticles were prepared from $Pd_2(dba)_3$, in the presence of an stabilizer, polymer **1** or ligand **2**, under hydrogen atmosphere in THF solution (Scheme 2) The reaction was stirred for 1 h at room temperature. The dibenzylidenacetone (dba) decoordination is therefore favored and partially reduced (dbaH). To eliminate the organic byproducts, the black residue was washed with hexane (monitored by TLC and $^1H$ NMR).

(44) Amatore, C.; Jutand, A.; Amine, M. *Organometallics* **1992**, *11*, 3009.

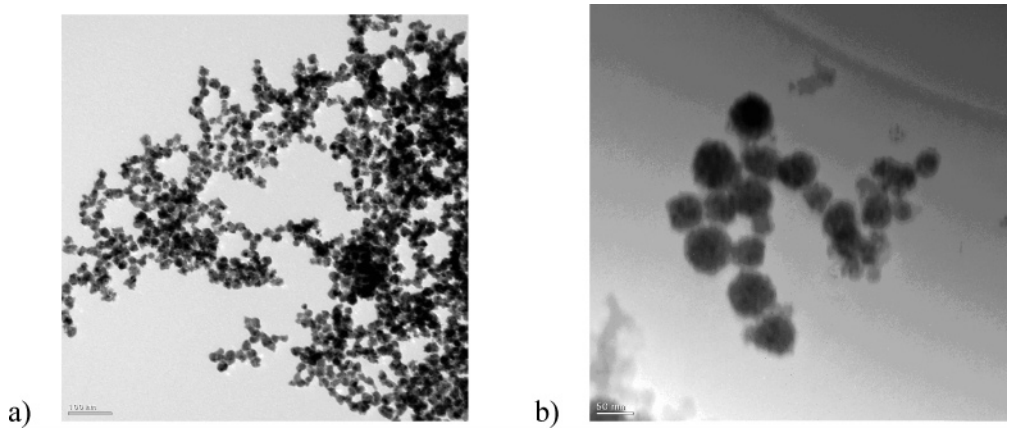

**Figure 1.** TEM micrographs of [Pd3] nanoparticles stabilized by polymer: (a) at the initial time (mean diameter, ca. 22 nm); (b) after 5 min (mean diameter, ca. 50 nm).

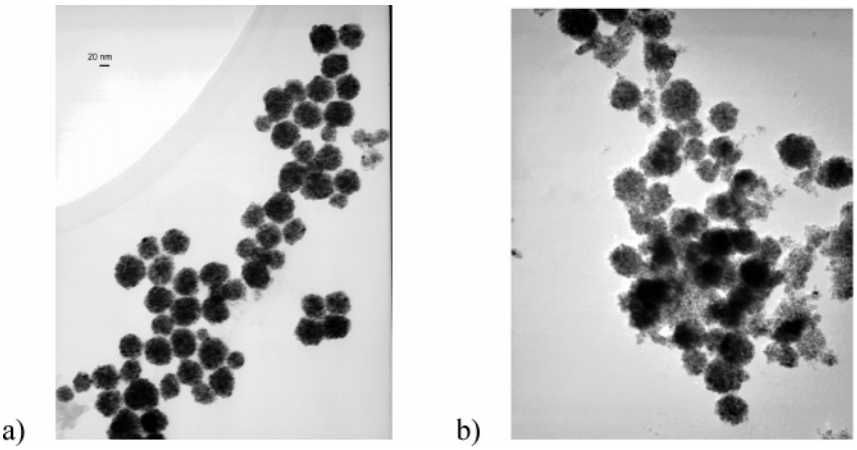

**Figure 2.** TEM micrographs of [Pd4] nanoparticles stabilized by ligand: (a) at the initial time (mean diameter, ca. 4 nm); (b) after 5 min (mean diameter, ca. 5 nm).

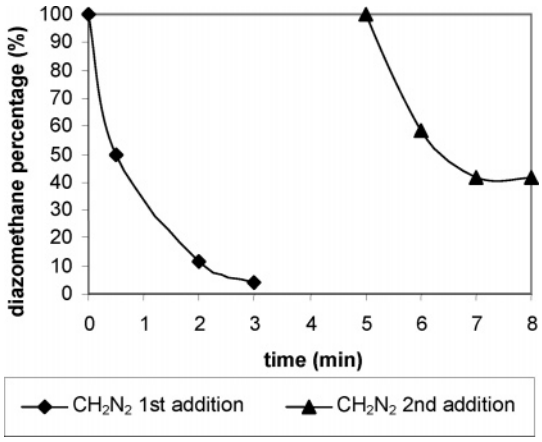


**Figure 3.** Variation of the diazomethane concentration with time in the presence of $Pd(OAc)_2$ at −80 °C.

their size with time from 6 to 13 nm. The formation of bulk metal was not observed in any case.

When a similar experiment was carried out at room temperature, 83% of cyclopropane **2** was obtained 1 min after the addition of cyclohexenone. The formed nanoparticles were bigger (estimated mean diameter ca. 40 nm) and considerably less active.

All these results point out the role of Pd nanoparticles in the cyclopropanation of cyclohexenone. These nanoparticles are formed from the reduction of $Pd(OAc)_2$ by diazomethane and remain stable and active during the reaction. These nanoparticles could act as catalysts themselves or as a reservoir of Pd(0) molecular species that would be the active catalysts of the reaction.

In order to analyze the oxidation state of palladium species in solution, we carried out cyclic voltammetry studies of the reaction mixture after cyclopropanation of **1**. The measurements were carried out in dichloromethane from −2 to +2 V (electrochemically stable solvent region) in the presence of tetrabutylammonium hexafluorophosphate as supporting electrolyte. No redox reactions of cyclohexanone **1** are expected in the studied region.[45] Free acetate (sodium acetate was measured) and 2-cyclohexen-1-one were not detected after cyclopropanation. To study the electrochemical behavior of Pd(0) and Pd(II) species under our conditions, $Pd_2(dba)_3$ and $Pd(OAc)_2$ were considered (Figure 6). For $Pd_2(dba)_3$, Pd(0) to Pd(II) oxidation appeared at +1.1 V (two peaks at −1.5 and −1.2 V were also observed due to dba reduction), according to published data.[46] The palladium acetate cyclovoltammogram showed two peaks corresponding to reduction processes, at +0.8 V (acetate reduction) and at −0.6 V (Pd(II) reduction).[47]

The solution mixture after cyclopropanation showed two peaks corresponding to irreversible reduction processes, at −1.0 and −1.6 V, and one oxidation peak at +0.8 V, for both

(45) House, H. O.; Prabhu, A. V.; Wilkins, G. M.; Lee, L. F. *J. Org. Chem.* **1976**, *41*, 3067.

(46) Amatore, C.; Broeker, G.; Jutand, A.; Khalil, F. *J. Am. Chem. Soc.* **1997**, *119*, 5176.

(47) (a) Amatore, C.; Blart, E.; Gênet, J. P.; Jutand, A.; Lemaire-Audoire, S.; Savignac, M. *J. Org. Chem.* **1995**, *60*, 6829. (b) Amatore, C.; Jutand, A.; M'Barki, M. A. *Organometallics* **1992**, *11*, 3009.

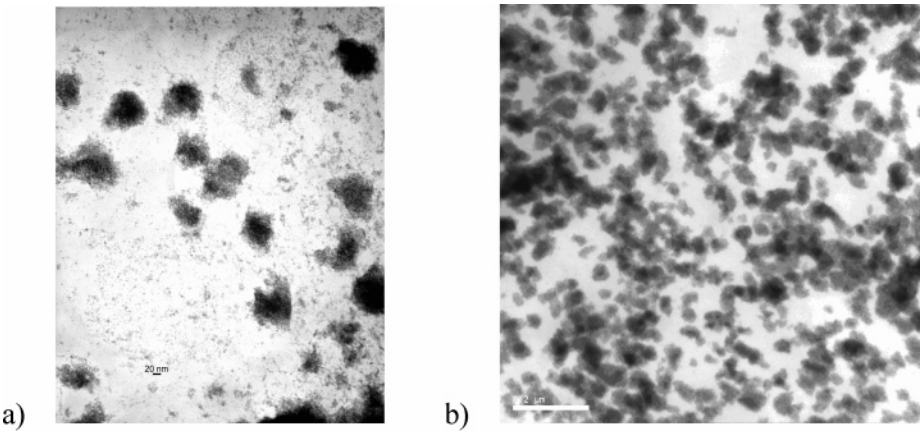


**Figure 4.** TEM micrographs after cyclohexenone cyclopropanation at room temperature: (a) using Pd/**1** = 1/1; (b) using Pd/**1** = 0.1/1.

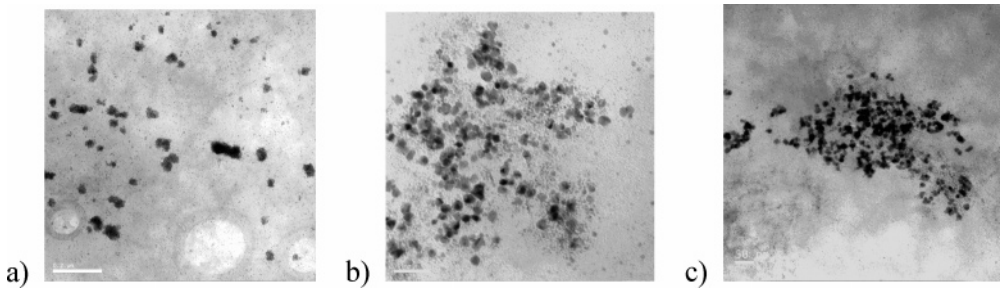


**Figure 5.** TEM micrographs: (a) after 1 min reaction time between $CH_2N_2$ and $Pd(OAc)_2$ (before addition of cyclohexenone), mean diameter, ca. 6 nm; (b) at 5 min reaction time between $CH_2N_2$ and $Pd(OAc)_2$ (before addition of cyclohexenone), mean diameter, ca. 10 nm; (c) after 8 min reaction time between $CH_2N_2$ and $Pd(OAc)_2$ (3 min after addition of cyclohexenone), mean diameter, ca. 13 nm. Reaction temperature = −80 °C.

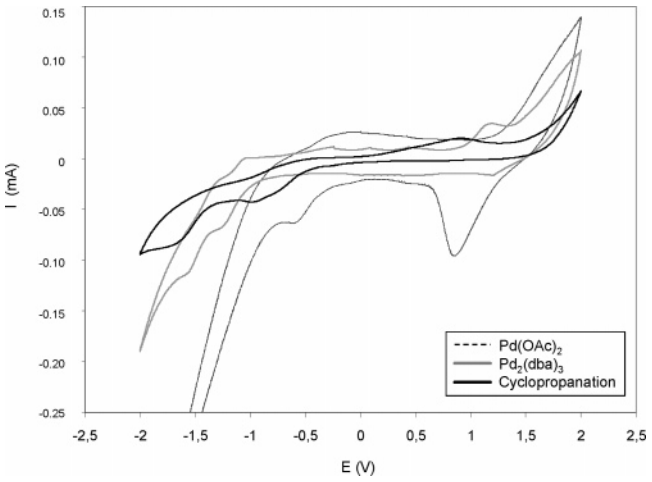


**Figure 6.** Cyclic voltammograms of $Pd(OAc)_2$, $Pd_2(dba)_3$, and solution mixture after cyclopropanation.

recorded voltammograms from −2 to +2 V and from +2 to −2V (Figure 6). The reduction peak at −1.0 V could be associated with a Pd(II) to Pd(0) process, in agreement with voltammograms of Pd(II) species. The oxidation observed at +0.8 V could be related to a Pd(0) to Pd(II) process, according to Pd(0) species voltammograms (see Figure 6 for $Pd_2(dba)_3$). The peak at −1.6 V could be due to the reduction of other metallic species.

It is noteworthy that Pd(0) species were still present in the reaction mixture after cyclopropanation was completed. In addition, the far-IR spectrum (400−200 $cm^{-1}$) of the residue obtained from the cyclopropanation solution after organic phase separation was measured and no absorption band was observed in the region 550−200 $cm^{-1}$, excluding the presence of palladium oxide (see the Supporting Information).[48]

From the results described up to now it is evident that, in the presence of diazomethane, palladium diacetate reduces to form Pd(0) species, probably small nanoparticles, which play a role in the cyclopropanation of cyclohexenone. However, the mechanism of Pd(II) to Pd(0) reduction remains unclear. With the purpose of its elucidation, we carried out a theoretical study concerning this process.

**2. Theoretical Study of the Pd(II) to Pd(0) Reduction.** In our previous work, we have shown that the formation of a bis(formyloxymethyl)palladium complex from the reaction of palladium dicarboxylate with two diazomethane molecules is very favorable.[34] Therefore, we have now started our investigation with a bis(acetyloxymethyl)palladium complex, which henceforth will be named **A(1)** (see below).

The Pd(II) to Pd(0) reduction mechanism involves many steps, which are summarized in Scheme 3. **A**, **B**, **C**, ..., refer to the kind of intermediate, whereas *n* refers to the number of methylene groups in the acetyloxyalkyl ligand on the right-hand side. In complexes **E** and **F** one of the methylene groups has become part of the C=C double bond of the alkene ligand.

The mechanism begins with an **A(*n*)** complex. The first two steps involve coordination of diazomethane and elimination of nitrogen to form a palladium−carbene complex **C(*n*)**. This intermediate may evolve following two different pathways. One of them leads to **A(*n*+1)**, which differs from **A(*n*)** in one methylene group and which can initiate another cycle. The alternative path leads to the formation of **F(*n*−1)**, which is a Pd(0) complex. We have studied these processes starting from

(48) Nakamoto, K. *Infrared and Raman Spectra of Inorganic and Coordination Compounds, PartB*; 5th ed.; Jonh Wiley & Sons: New York, 1997.

**Scheme 3**

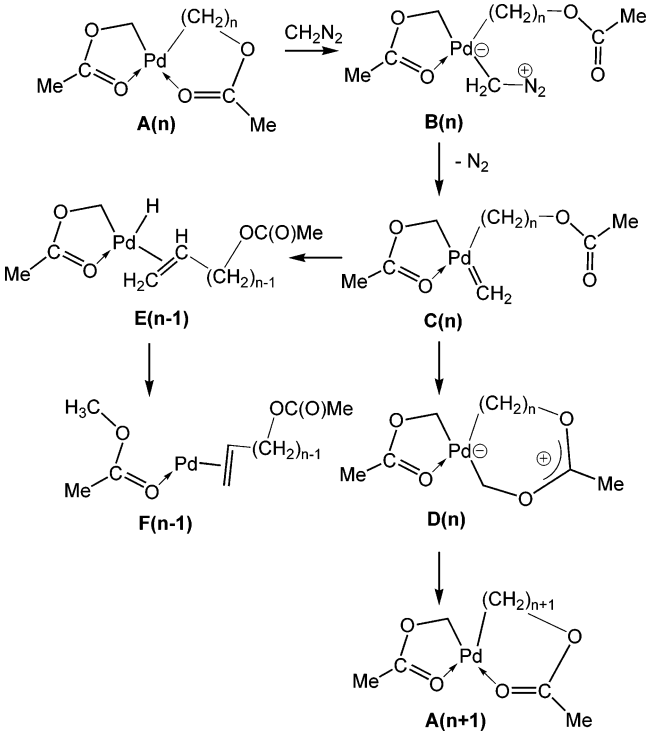


**Scheme 4**

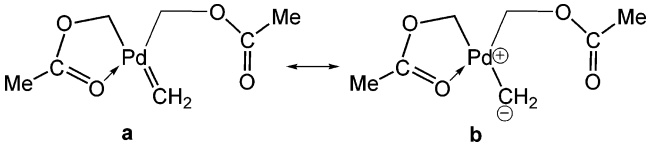


**A(1)** and from **A(2)**. The formation of a Pd(0) complex is favored only for the second cycle, which leads to **F(1)**.

Table 2 presents the computed Gibbs activation and reaction energies of the processes that originate in **A(1)**, and the structures of selected stationary points are shown in Figures 7 and 8.

Figure 7 shows the structures of the intermediates involved in the reaction between **A(1)** and diazomethane. The coordination of diazomethane to **A(1)** leads to the formation of **B(1)**, which loses nitrogen, leading to the palladium−carbene complex **C(1)**. Two different transformations are possible for **C(1)**, as summarized in Scheme 3. The structures of the corresponding stationary points are shown in Figure 8.

**C(1)** may evolve to **D(1)** through the formation of a C−O bond between the coordinated methylene and the terminal oxygen of the acetyloxymethyl ligand.

Alternatively, **C(1)** may undergo a C−C coupling between the methylene ligand and the methylene group of the *cis* acetyloxymethyl ligand along with a α-hydride elimination leading to the formation of the olefin−hydride complex **E(0)**. This complex easily evolves to the **F(0)** through a C−H reductive elimination involving the acetyloxymethyl ligand. This is a Pd(0) complex with vinyl acetate and methyl acetate ligands.

The most favorable process for **C(1)** is its evolution to **D(1)** ($\Delta G^{\ddagger} = 2.9$ kcal mol$^{-1}$ in dichloromethane). However, **D(1)** is unstable and rapidly evolves to **A(2)**, through the cleavage of one of the $CH_2$−O bonds and a C−C coupling. Figure 8 shows the most stable conformer of **A(2),** but the evolution from **D(1)** leads first to the **A(2)′** conformer (see Figure 9), which is 7.6 kcal mol$^{-1}$ higher in Gibbs energy than **A(2)**. The Gibbs

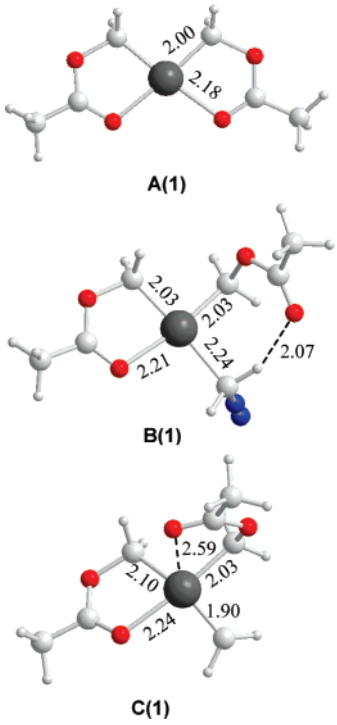


**Figure 7.** Structures of **A(1)** and intermediates involved in the reaction with diazomethane. Selected interatomic distances are in Å.

**Table 2. Gibbs Activation and Reaction Energies (in kcal mol$^{-1}$)[a] for Reactions Shown in Scheme 3**

| | $\Delta G^{\ddagger}$ | $\Delta G°$ |
|---|---|---|
| **A(1)** + $CH_2N_2$ → **B(1)** | 19.3 | 10.5 |
| **B(1)** → **C(1)** + $N_2$ | 17.6 | 2.3 |
| **C(1)** → **D(1)** | 2.9 | −11.3 |
| **D(1)** → **A(2)** | 5.4 | −47.3 |
| **C(1)** → **E(0)** | 3.9 | −35.1 |
| **E(0)** → **F(0)** | 8.0 | −5.2 |

[a] In dichloromethane at 298 K and 1 mol L$^{-1}$.

activation energy for the conformational rearrangement is 4.6 kcal mol$^{-1}$. The global process starting from **C(1)** can be viewed as the methylene insertion into the $CH_2$−O bond of the *cis* acetyloxymethyl ligand.

The electronic structure of complexes shown in Figures 7 and 8 has been studied using the NBO method. Table 3 presents the Pd net charges and the number of 4d lone pairs on Pd identified by the NBO procedure. Three different situations emerge. In most of the complexes, the net charge on Pd is in the 0.35−0.46 range and there are four 4d lone pairs on Pd. These complexes correspond to Pd(II). In **C(1)** the net charge on Pd is notably larger and there are only three 4d lone pairs on Pd, which fits to a Pd(IV) complex. Moreover, the NBO procedure identifies only a $\sigma$ bond between Pd and methylene and a p lone pair on the methylene carbon atom. This result points to a resonant structure **b** for **C(1)** (see Scheme 4). As a matter of fact, the methylene group in **C(1)** is slightly pyramidal, with a sum of bond angles around the carbon atom of 351.4°. Finally, the results obtained for **F(0)** show that it is a Pd(0) complex.

**A(2)** may be the origin of the same kind of transformations as **A(1)**. Table 4 presents the computed Gibbs activation and reaction energies. **A(2)** may coordinate a new diazomethane molecule, and two different isomers of the corresponding complex diazomethane−**A(2)** can be formed (see Figure 10). The coordination on the side of the acetyloxyethyl ligand is

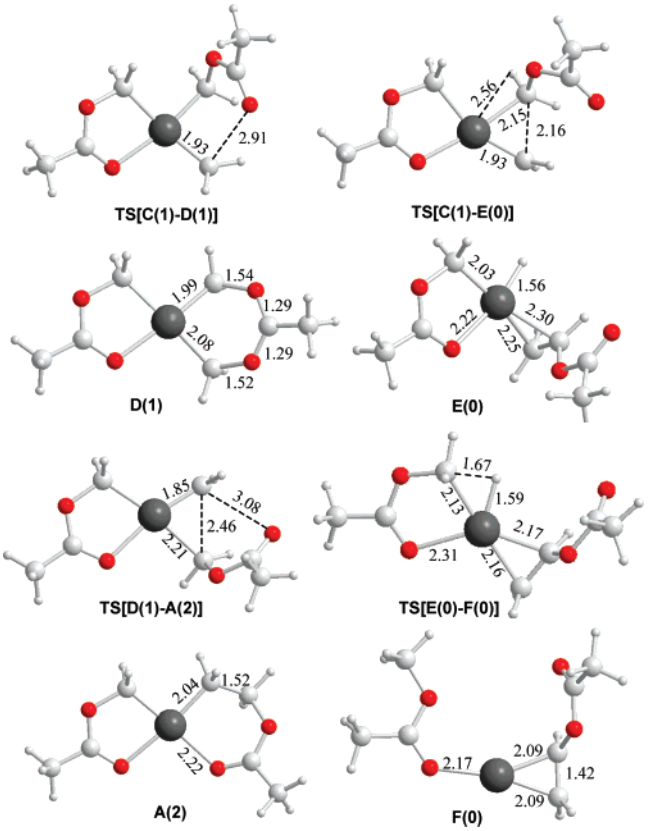


**Figure 8.** Structures of stationary points corresponding to rearrangements from **C(1)**. Selected interatomic distances are in Å.

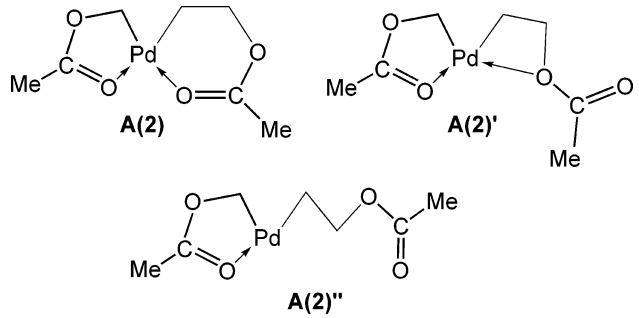


**Figure 9.** Structures of conformers **A(2)**, **A(2)′**, and **A(2)″**.

**Table 3. Net Charge (*Q*, in au) on Pd and Number of Pd 4d Lone Pairs (LP) from the NBO Analysis of Complexes Shown in Figures 7 and 8**

| | *Q* | LP |
|---|---|---|
| **A(1)** | 0.458 | 4 |
| **B(1)** | 0.398 | 4 |
| **C(1)** | 0.674 | 3 |
| **D(1)** | 0.415 | 4 |
| **A(2)** | 0.449 | 4 |
| **E(0)** | 0.348 | 4 |
| **F(0)** | 0.160 | 5 |

thermodynamically more favorable (**B(2)**, $\Delta G = 5.4$ kcal mol$^{-1}$) than the coordination on the side of the acetyloxymethyl ligand (**B(2)′**, $\Delta G = 12.0$ kcal mol$^{-1}$).

The coordination on the side of the acetyloxyethyl ligand may take place after a conformational rearrangement in which this ligand adopts an extended disposition, leaving a free coordination site in Pd (**A(2)″** in Figure 9). This process involves a Gibbs activation energy of 13.2 kcal mol$^{-1}$ and a Gibbs reaction energy of 4.9 kcal mol$^{-1}$. Then the coordination of diazomethane takes

**Table 4. Gibbs Activation and Reaction Energies (in kcal mol$^{-1}$)[a] for Reactions Shown in Scheme 3**

| | $\Delta G^{\ddagger}$ | $\Delta G°$ |
|---|---|---|
| **A(2)** + $CH_2N_2$ → **B(2)** | 16.5 | 5.4 |
| **A(2)** + $CH_2N_2$ → **B(2)′** | 19.8 | 12.0 |
| **B(2)** → **C(2)** + $N_2$ | 17.2 | 2.2 |
| **C(2)** → **D(2)** | 8.2 | 1.5 |
| **D(2)** → **A(3)** | 2.9 | −53.0 |
| **C(2)** → **E(1)** | 5.1 | −43.5 |
| **E(1)** → **F(1)** | 7.6 | −6.1 |

[a] In dichloromethane at 298 K and 1 mol L$^{-1}$.

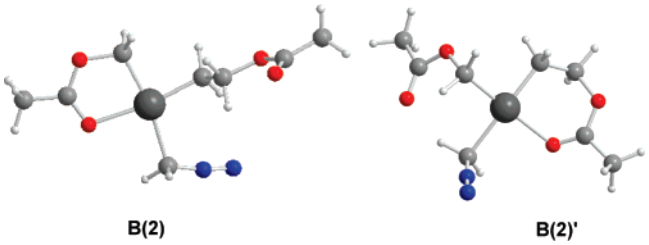


**Figure 10.** Structure of complexes containing **A(2)** and diazomethane.

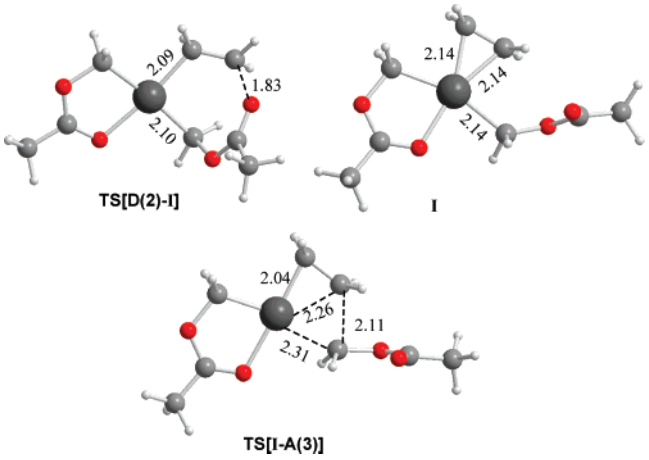


**Figure 11.** Structures of stationary points corresponding to the **D(2)** to **A(3)** rearrangement. Selected interatomic distances are in Å.

place with no energy barrier. We have optimized the geometry for different values of the Pd−diazomethane distance in the range between 3.6 and 3.0 Å. These structures present an imaginary frequency corresponding to the approach of both fragments. The frequencies have been projected for vibrations perpendicular to the path, and the Gibbs energies have been calculated. The Gibbs energy presents a maximum for R = 3.5 Å, from which we have computed the Gibbs activation energy relative to the most stable structure of **A(2)** of 16.5 kcal mol$^{-1}$.

An alternative reaction pathway for **A(2)** would be a $\beta$-hydride elimination to form an isomer of **E(0)** with the hydride *trans* relative to the methylene group of the acetyloxymethyl ligand. The corresponding Gibbs activation and reaction energies are 22.2 and 21.1 kcal mol$^{-1}$, respectively. Therefore, this process is less favorable than the coordination of diazomethane to **A(2)** (see Table 4). **E(0)** could be reached from the *trans* isomer of **A(2)**, which is 20.1 kcal mol$^{-1}$ higher in Gibbs energy; consequently the process is not expected to be favorable.

**C(2)** may undergo the same kind of rearrangements as **C(1)**. The **D(2)** to **A(3)** rearrangement takes place in two steps through an intermediate **I**, as shown in Figure 11. The first step consists in the cleavage of the C−O bond involving the $\beta$ methylene group and leads to the formation of an (ethylene)(acetyloxym-

**Scheme 5**

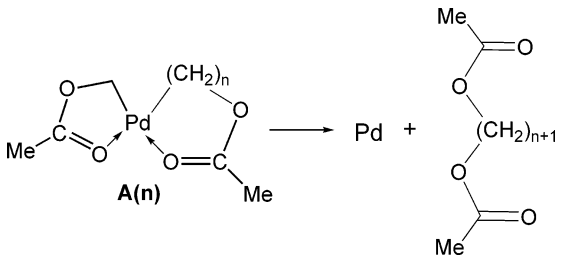


**Table 5. Gibbs Activation and Reaction Energies (in kcal mol$^{-1}$)[a] for Alkyl Diacetate Reductive Elimination from A(n) Complexes**

| | $\Delta G^{\ddagger}$ | $\Delta G^{\circ}$ |
|---|---|---|
| **A(1)** | 51.9 | 38.4 |
| **A(2)** | 45.9 | 30.2 |
| **A(3)** | 39.0 | 22.9 |

[a] In dichloromethane at 298 K and 1 mol L$^{-1}$.

ethyl)Pd complex with a Gibbs activation energy of 2.9 kcal mol$^{-1}$ and a Gibbs reaction energy of −34.3 kcal mol$^{-1}$. The second step is the insertion of ethylene into the Pd−$CH_2$ bond, and the Gibbs activation and reaction energies are 13.9 and −18.3 kcal mol$^{-1}$, respectively.

The rearrangement from **C(2)** to **E(1)** is now kinetically more favorable than the rearrangement to **D(2)**, in contrast with the results obtained for **C(1)**. So, the final product would be **F(1)**, which is a Pd(0) complex.

The Gibbs reaction energies for the dissociation of methyl acetate and allyl acetate ligands from **F(1)** are −5.3 and 27.6 kcal mol$^{-1}$, respectively, so that the dissociation of the methyl acetate ligand is favorable. The subsequent dissociation of the allyl acetate ligand to form a bare Pd atom involves a Gibbs reaction energy of 40.4 kcal mol$^{-1}$. However, the process could be facilitated by the formation of Pd aggregates.

In addition to **F(*n*)** complexes Pd(0) could also be obtained from reductive elimination of alkyl diacetates from **A(*n*)** complexes (see Scheme 5). We have studied this process for **A(1)**, **A(2)**, and **A(3)**. The computed Gibbs activation and reaction energies are shown in Table 5.

Reductive elimination is unfavorable, but becomes more feasible as the number of methylene units increases. However, the Gibbs activation energies are much larger than those corresponding to the coordination of an additional diazomethane molecule, so that it does not seem to be the mechanism of reduction.

Up to now we have shown how palladium diacetate may evolve to Pd(0) in the presence of diazomethane. The proposed mechanism involves as intermediates palladium−carbene complexes, which would participate in a Pd(II)-catalyzed cyclopropanation. To elucidate the feasibility of this mechanistic pathway, we have studied the reaction between one of them, **C(1)**, and cyclohexenone. We have located the transition state for the cyclopropanation, and the computed Gibbs activation energy in dichloromethane is 13.0 kcal mol$^{-1}$. This value is notably higher than the Gibbs activation energies associated with the two intramolecular rearrangements considered for **C(1)** (see Table 2), so that in the presence of cyclohexenone the Pd(II)/Pd(0) reduction is more favorable than Pd(II)-catalyzed cyclopropanation. Similar values of Gibbs activation energies are expected for the reactions of cyclohexenone with other palladium−carbene complexes, such as **C(2)**, since the major contribution comes from the entropy variation associated with the molecularity change. On the other hand, the alternative rearrangement paths are always unimolecular processes. These results allow us to discard the catalysis by Pd(II) complexes in the cyclopropanation process.

The results of calculations show that the most favorable Pd(II) to Pd(0) reduction path would lead to the formation of methyl acetate and allyl acetate. On the contrary, vinyl acetate is not expected to be formed. All these predictions are confirmed by the experimental results. Other products detected by mass spectrometry come from oligomerization of such monomers under the reaction conditions used.

## Concluding Remarks

$Pd(OAc)_2$ rapidly decomposes in the presence of diazomethane, leading to the formation of Pd(0) nanoparticles, which are active for the catalytic diazomethane-mediated cyclopropanation of cyclohexenone. To our knowledge, this is the first time that evidence and a description are provided for Pd(0) nanoparticles formed under the catalytic conditions of the $Pd(OAc_2)$-promoted cyclopropanation reactions. These nanoparticles may act as catalysts themselves or as a reservoir of Pd(0) molecular species, which would be the active catalysts. The reactivity of the palladium nanoparticles depends on their size (in general, the smallest particles are the most active due to their high specific surface) and the nature of stabilizers (the presence of strong Lewis donor centers can poison the catalyst). These nanoparticles generated in situ are more active than Pd(0) complexes, preformed nanoparticles, and commercial palladium powder.

Moreover, we have shown that the Pd(II) to Pd(0) reduction mechanism involves the formation of methyl and allyl acetates, and oligomers coming from them, which have been identified by mass spectrometry.

## Experimental Section

**Computational Details.** All calculations are based on the density functional theory using the BPW91 functional,[51,52] which is the functional used in previous studies.[32,34] Geometries have been fully optimized using the LANL2DZ basis set supplemented with d polarization functions for C, N, and O. This basis set uses effective core potentials for Pd[51] and the D95 basis set for the remaining atoms.[52] Harmonic vibrational frequencies have been computed for all structures to characterize them as energy minima or transition states. The electronic structure of several complexes has been analyzed using the NBO method.[53] Solvent effects have been taken into account for geometries optimized in the gas phase using the PCM method[54] and using dichloromethane ($\epsilon = 8.93$) as solvent. All these calculations have been done using the Gaussian-03 program.[55] The energies of all structures have been recomputed through single-point calculations with the ADF program[56] using

(49) Becke, A. D. *Phys. Rev. A* **1988**, *38*, 3098.
(50) (a) Wang, Y.; Perdew, J. P. *Phys. Rev. B* **1991**, *44*, 13298. (b) Perdew, J. P.; Chevary, J. A.; Vosko, S. H.; Jackson, K. A.; Pederson, M. R.; Singh, D. J.; Fiolhais, C. *Phys. Rev. B* **1992**, *46*, 6671.
(51) Hay, P. J.; Wadt, W. R. *J. Chem. Phys.* **1985**, *82*, 299.
(52) Dunning, T. H.; Hay, P. J. *Modern Theoretical Chemistry, Vol. 3*; Schaeffer, H. F., III, Ed.; Plenum: New York, 1976; p 1.
(53) Reed, A. E.; Curtiss, L. A.; Weinhold, F. *Chem. Rev.* **1988**, *88*, 899.
(54) (a) Miertus, S.; Scrocco, E.; Tomasi, J. *J. Chem. Phys.* **1981**, *55*, 117. (b) Cancès, E.; Menucci, B.; Tomasi, J. *J. Chem. Phys.* **1997**, *107*, 3032.
(55) Frisch, M. J.; et al. *Gaussian 03*, Revision C.02; Gaussian, Inc.: Wallingford, CT, 2004.
(56) (a) te Velde, G.; Bickelhaupt, F. M.; Baerends, E. J.; Fonseca Guerra, C.; van Gisbergen, S. J. A.; Snijders, J. G.; Ziegler, T. *J. Comput. Chem.* **2001**, *22*, 931. (b) *ADF2005.01*, *SCM*; Theoretical Chemistry, Vrije Universiteit, Amsterdam: The Netherlands, http://www.scm.com.

an uncontracted Slater orbital TZ2P basis set. The inner electrons of Pd (up to the 3d shell), C, N, and O have been treated with the frozen core approximation.[57] Relativistic effects have been included using the ZORA method.[58] The reference state for the reported Gibbs energies in solution is 298.15 K and 1 mol $L^{-1}$.

**Cyclic Voltammetry Studies.** Experiments were carried out in a three-electrode cell. The auxiliary electrode was a stirring platinum disk electrode (2 mm diameter); the reference electrode was a Ag/AgCl electrode, and the working electrode, a platinum wire. The cyclic voltammetry was performed at a scan rate of 0.1 V/s, and 0.1 M $NBu_4^+PF_6^-$ was used as supporting electrolyte. Dichloromethane solutions from a catalytic mixture, $Pd(OAc)_2$ (80 mg, mmol), $Pd_2(dba)_3$ (80 mg, mmol), and cyclohexenone (25 mg, mmol) in 10 mL of solvent were measured. Redox-potential values were confirmed by measuring solutions at different concentrations.

**Pd Nanoparticle Synthesis.** To a solution of $Pd_2(dba)_3$ (10 mg, 0.011 mmol) in 50 $cm^3$ of distilled and degassed THF in a Fischer-Porter bottle was added a solution of polymer **3** (139 mg, 0.44 mmol; monomer/palladium = 20) or ligand **4** (1.65 mg, $4.4 \times 10^{-2}$ mmol). The mixture was then pressurize at 3 bar of hydrogen at room temperature and stirred for 1 h. During this time the solution color changed from violet to black, with formation of a colloidal suspension. The mixture was then depressurized under nitrogen atmosphere and the solvent removed under reduced pressure. The residue was then washed with hexane ($6 \times 15$ mL) to eliminate dba and its reduced products (monitored by TLC). The black solid obtained was dried under reduced pressure. Analysis for $[Pd\mathbf{3}]_{coll}$: Anal. Found: C, 49.71; H, 9.15; N, 7.42; S, 1.47; Pd, 10.55. Mean diameter (TEM, nm): 22. Analysis for $[Pd\mathbf{4}]_{coll}$: Anal. Found: C, 39.25; H, 6.13; N, 0.41; Pd, 42.14. Mean diameter (TEM, nm): 4.

**General Cyclopropanation Procedure.** Cyclohexenone (25 mg, 0.26 mmol) and $Pd(OAc)_2$ (5.84 mg, 0.026 mmol) were introduced in an Erlenmeyer vessel, and then a 0.2 M solution of diazomethane in dichloromethane (26 mL, 5.2 mmol) was added. The mixture was stirred for 5 min at room temperature. Immediately a $N_2$ leak and a color change of the solution, brown to gray, were observed. The reaction progress was monitored by GC using authentic samples of cyclohexenone **1** and cyclopropane **2** as external standards.

**Kinetic Studies.** A solution of 0.12 M diazomethane in dichloromethane (21 mL, 2.52 mmol) was added to a flask containing $Pd(OAc)_2$ (29 mg, 0.13 mmol) and cooled at −80 °C by an external bath. The mixture was stirred for 5 min at −80 °C. The concentration of diazomethane at different reaction times was determined by addition of a known amount of benzoic acid to reaction aliquots, and the excess of benzoic acid was then titrated with 0.2 M aqueous NaOH.

**Acknowledgment.** The authors wish to thank the Ministerio de Educació y Ciencia (CTQ 2004-1067/BQU and CTQ2004-1546/BQU), the Generalitat de Catalunya, and the CNRS (France) for financial support. Access to computational facilities of Centre de Supercomputació de Catalunya (CESCA) is gratefully acknowledged.

**Supporting Information Available:** Cyclic voltammograms of $Pd_2(dba)_3$ and $Pd(OAc)_2$. Far-IR spectrum of the residue obtained from the cyclopropanation solution. Cartesian coordinates and total energies for all structures obtained from theoretical calculations. This material is available free of charge via the Internet at http://pubs.acs.org.

OM070141A

(57) Baerends, E. J.; Ellis, D. E.; Ros, P. *Chem. Phys.* **1973**, *2*, 41.

(58) (a) van Lenthe, E.; Baerends, E. J.; Snijders, J. G. *J. Chem. Phys.* **1993**, *99*, 4597. (b) van Lenthe, E.; Baerends, E. J.; Snijders, J. G. *J. Chem. Phys.* **1994**, *101*, 9783. (c) van Lenthe, E.; Snijders, J. G.; Baerends, E. J. *J. Chem. Phys.* **1996**, *105*, 6505. (d) van Lenthe, E.; van Leeuwen, R.; Baerends, E. J.; Snijders, J. G. *Int. J. Quantum Chem.* **1996**, *57*, 281. (e) van Lenthe, E.; Ehlers, A. E.; Baerends, E. J. *J. Chem. Phys.* **1999**, *110*, 8943.